Single-active-electron ionization of C_{60} in intense laser pulses to high charge states

A. Jaroń-Becker
Institut für Physikalische Chemie und Elektrochemie, Technische Universität Dresden, D-01062 Dresden, Germany

A. Becker
Max-Planck-Institut für Physik komplexer Systeme, Nöthnitzer Strasse 38, D-01187 Dresden, Germany

F. H. M. Faisal
Fakultät für Physik, Universität Bielefeld, Postfach 100131, D-33501 Bielefeld, Germany and ITAMP, Harvard-Smithsonian Center for Astrophysics, 60 Garden Street, Cambridge, Massachusetts 02138

(Received 14 November 2006; accepted 6 February 2007; published online 26 March 2007)

Sequential ionization of the C_{60} fullerene to high charge states in ultrashort intense laser pulses is investigated within the strong-field *S*-matrix approach. Ion yields are calculated and saturation intensities are determined for a broad range of laser wavelengths between 395 and 1800 nm at different pulse lengths. Comparisons of the *S*-matrix predictions for the saturation intensities with recent experimental data are in an overall satisfactory agreement, indicating that saturation of ionization of this complex molecule can be well described using the single-active-electron approach. The analysis of the results shows that the contributions from the h_u-highest occupied molecular orbital to the ion yields dominate as compared to those from the inner valence shells h_g and g_g. Finally, it is demonstrated that the suppression of ionization of C_{60} and its ions, as observed in experiments, can be interpreted within the present theory as due to the finite cage size of the fullerenes and a multi-slit-like interference effect between partial waves emitted from the different nuclei of the fullerenes. © *2007 American Institute of Physics*. [DOI: 10.1063/1.2712844]

I. INTRODUCTION

The interaction of complex molecular systems with an intense ultrashort laser pulse is currently a subject of active research in view of a potential control of electronic and nuclear rearrangements on ultrashort time scales (e.g., Refs. 1–3). One of the reasons why the physical mechanisms behind the control remain often obscure is the still limited knowledge about ionization and fragmentation pathways of large molecules in an intense field. While the dynamical aspects of laser induced ionization of noble gas atoms in a strong laser field are considered to be well understood, much less theoretical analysis of the same process in more complex targets, such as diatomic and polyatomic molecules and clusters, has been performed.

The nonlinear interaction of hydrogen and noble gas atoms with an intense field is mainly dominated by a dynamical single-active-electron (SAE) response, as it has been shown in many theoretical studies using *ab initio* numerical simulations (e.g., Refs. 4 and 5), Floquet calculations (e.g., Refs. 6 and 7), tunneling models,[8–10] or *S*-matrix theories, such as the Keldysh-Faisal-Reiss (KFR) model.[8,11,12] Quantitative agreement between theoretical predictions and experimental data for the total single ionization yields over a wide range of wavelengths, pulse durations, and peak intensities as well as linear and circular polarization has been found.[13,14] Even simple tunneling formulas[9,10] provide good estimates of the ionization rates of atomic gases at high intensities and are often used to determine the saturation intensities of noble gas atoms.[15–17] The SAE dynamics can be readily understood from the basic fact that the fundamental interaction of photons with a many-electron system is given by the independent sum of *one-electron* interactions (e.g., in dipole length gauge, $V(t)=\Sigma_{i=1}^{n_e}\boldsymbol{E}(t)\cdot\boldsymbol{r}_i$, where $\boldsymbol{E}(t)$ is the electric field, $\boldsymbol{r}_i$ is the coordinate of the ith electron, and n_e is the number of electrons, e.g., in the valence shell of the atom). Many-electron effects, mediated via the electron-electron interaction, are found to contribute to processes such as nonsequential double ionization, but at a lower rate (e.g., Refs. 18–21).

Results of early measurements of ion yields of diatomic molecules at the long wavelengths of CO_2 lasers[22–25] were nearly identical to those of the companion atoms, which have comparable ionization potentials. This similarity of the ionization yields has been thought to be a consequence of the tunneling ionization, in which the ionization probability depends on the ionization potential and the field strength only. More recent works using Ti:sapphire laser systems and/or larger molecules, however, have shown that this early interpretation does not hold. Simple diatomics as well as complex molecules do reach, in general, with a few exceptions, saturated ionization at higher intensities than it is expected for companion atoms.[16,26,27] One of the basic questions regarding this observation is whether the response of large molecules is still dominated by a dynamical single-active-electron response or multielectron mechanisms become active.

The ionization of C_{60} fullerenes to high charge states using intense laser pulses has raised considerable interest re-

cently (for a recent review, see Ref. 28). C_{60} is an example of a complex molecule with a high symmetry and a well defined electronic structure.[29] With its 240 valence electrons, of which 60 form a delocalized π-electron system while 180 are structure defining localized σ electrons, it constitutes an interesting prototype to study many-electron effects in large molecules. The experimental observation of unexpectedly high saturation intensities of the C_{60} fullerene and its multiply charged ions at long laser wavelengths in the tunneling regime[27] has been first interpreted as a failure of the SAE hypothesis.[27,30,31] Instead a multi-electron picture including field-induced polarization effects[27,30] and a many-electron angular momentum barrier[31] has been put forward. But recently, we have shown[32] that the same experimental saturation intensities can be also well reproduced within a single-active-electron theory, namely, an extension of the well-known KFR theory for atoms[8,11,12] to the molecular case. In our analysis we have found that the suppression of the ionization is induced by the finite cage size of the C_{60} fullerene and a multi-slit-like interference effect between partial waves emitted from the different nuclei of the fullerene. We have further predicted that the same effects of suppression of ionization should appear in other icosahedral fullerenes as well.

The aim of this paper is to test the predictions of the theory for the saturation intensities of C_{60} and its ions against the experimental data by Hertel and co-workers[28,33–35] obtained at shorter wavelengths, namely, the Ti:sapphire wavelength and its second harmonic. The paper is organized as follows. In Sec. II we give an outline of the extension of the KFR model for atoms to the fullerene case, taking into account the structural symmetry of the molecule, its finite cage size, the multicenter nuclear positions in the molecule, and the Coulomb correction of the outgoing Volkov plane wave in the KFR theory. In Sec. III we first compare the present theoretical predictions for the relative ion yields with the corresponding experimental data at different pulse lengths. Next, we investigate inner-valence shell contributions to the ion yields. In order to analyze the experimental data for the saturation intensities we investigate and compare different techniques to obtain saturation intensities. Finally, we apply the present theory to obtain the saturation intensities of C_{60} and its higher charge states at different wavelengths. The theoretical results are compared with the experimental data and analyzed in view of the finite cage size and multi-slit interference effects. We conclude with a brief summary.

II. THEORY

For our study we have used the lowest order S-matrix theory, namely, the well-known KFR model,[8,11,12] which accounts nonperturbatively for the intense-field interaction. We do not repeat the derivation of the general KFR amplitude here, which can be found in many articles (for a recent review on S-matrix theory, see, e.g., Ref. 19), but emphasize the modifications and generalizations of the standard KFR amplitude and rate formula for atoms to the fullerene case. The first-order KFR term of the intense-field S-matrix expansion arises from the transition of a single-active electron from the initial bound state into a final field-dressed plane-wave state (or Volkov state).[36] It can be written in velocity gauge as (Hartree atomic units, $e=m=\hbar=1$, are used)

$$S_{fi}^{(1)}(t_f,t_i) = -i\int_{t_i}^{t_f} dt_1 \langle \phi_V(\boldsymbol{k},\boldsymbol{r}_1,t_1)\phi_f(\boldsymbol{r}_2\ldots\boldsymbol{r}_m,\boldsymbol{R}_1\ldots\boldsymbol{R}_n,t_1)| -\frac{\hat{\boldsymbol{p}}_1\cdot\boldsymbol{A}(t_1)}{c}+\frac{A^2(t_1)}{2c^2}|\phi_i(\boldsymbol{r}_1\ldots\boldsymbol{r}_m,\boldsymbol{R}_1\ldots\boldsymbol{R}_n,t_1)\rangle. \quad (1)$$

$\hat{\boldsymbol{p}}_1$ is the momentum operator of the active electron, $\phi_V(\boldsymbol{k},\boldsymbol{r},t)$ is the Volkov wave function of momentum $\boldsymbol{k}$ (Ref. 36) and $\boldsymbol{A}(t)$ is the vector potential of the field. ϕ_i and ϕ_f are the undressed initial and final state wavefunctions of the fullerene and its ions. We have found in test calculations that, in general, the contributions from the nonactive electrons $2,\ldots,m$ can be neglected in the overlap matrix element between the initial and final state wavefunctions. This is supposedly due to the fact that the corresponding many-electron molecular orbitals do not change significantly by the removal of one electron from the fullerene. We therefore drop the corresponding contributions in the equations below, as well as in the present calculations, and represent the molecular orbital of the active electron in the initial state as a linear combination of atomic orbitals, $\phi_{l,j}$, centered at the nuclear positions, $\boldsymbol{R}_l, l=1,2,\ldots,n$, e.g.,

$$\phi_i(\boldsymbol{r},\boldsymbol{R}_1,\ldots,\boldsymbol{R}_n,t) = \sum_{l=1}^{n}\sum_{j=1}^{j_{\max}} a_{l,j}\phi_{l,j}(\boldsymbol{r},\boldsymbol{R}_l)\exp(-iE_it), \quad (2)$$

where n is the total number of nuclei in the molecule, $a_{l,j}$ are the variational coefficients of the atomic basis functions $\phi_{l,j}$, and $j_{\max}$ is the size of the basis set used. The geometrical structure of the fullerene is obtained using the density-functional tight-binding (DFTB) method,[38–40] which allows for efficient quantum simulations of molecular systems containing several hundreds or thousands of atoms. In the calculations we have considered icosahedral symmetry for the fullerene as well as its cations, assuming that the geometrical structure of the atomic cage does not change during the ionization process. The mean radius of the fullerene cage from the present DFTB calculations was 6.74 a.u. The orbitals are obtained using the self-consistent Hartree-Fock method with Gaussian basis functions.[37] Thus, the amplitude in Eq. (1) takes direct account of the icosahedral structural symmetry, the finite size of the atomic "cage," the multicenter nuclear positions, and the angular momentum of the initial state of the C_{60} fullerene (or, in the same way, of the structure of any other molecule). Since the first-order term of the S-matrix expansion presents a direct transition from the initial bound state to the final Volkov state, it does not take account of resonances during the ionization process. The influence of intermediate electronically excited states on the process can be studied via the higher-order terms of the S-matrix expansion, which is beyond the scope of the present work.

Performing the time integral in Eq. (1) analytically and modulo squaring the resulting expression we obtain the probability of ionization per unit time or the basic rate as an analytical formula (for the derivation see, e.g., Ref. 19),

$$\Gamma^{+}(I) = 2\pi N_e C^2(Z,E_B,F) \times \sum_{N=N_0}^{\infty} \int d\hat{\mathbf{k}}_N k_n (U_p - N\omega)^2 J_N^2\left(\boldsymbol{\alpha}_0 \cdot \boldsymbol{k}_N, \frac{U_p}{2\omega}\right) \times \left| \sum_{l=1}^{n} M_l(\mathbf{k}_N;\boldsymbol{R}_l) \right|^2, \quad (3)$$

where

$$M_l(\mathbf{k}_N;\boldsymbol{R}_l) = \sum_{j=1}^{j_{\max}} a_{l,j} \langle \phi_0(\boldsymbol{k}_N,\boldsymbol{r}) | \phi_{l,j}(\boldsymbol{r},\boldsymbol{R}_l) \rangle \quad (4)$$

is the partial amplitude of the bound-free matrix element (or Fourier transform) of the molecular orbital at the lth nuclear center. The angle brackets stand for spatial volume integration. N_e is the number of equivalent electrons in the active molecular orbital [usually the highest occupied molecular orbital (HOMO)] of the molecule and E_B is the ionization potential to release an electron from the active orbital of the molecule, which have been taken from Refs. 29 and 41. $U_p = I/4\omega^2$ is the cycle-averaged kinetic energy of a free electron in a linearly polarized laser field of intensity $I=F^2$, where F is the field amplitude, and frequency ω, also known as ponderomotive or quiver energy. $k_N = \sqrt{2(N\omega - E_B - U_p)}$ is the momentum of the Volkov electron on absorbing N photons and $\phi_0(\boldsymbol{k}_N,\boldsymbol{r})$ is the plane wave of momentum k_N. N_0 is the minimum number of photons required for emission of the electron. $J_n(a;b)$ is the generalized Bessel function of two arguments, and $\alpha_0 = \sqrt{I}/\omega^2$ is the "quiver radius" of oscillations of a free electron.

It should be noted that the rate in Eq. (3) differs from the original KFR rate not only by its generalization to the molecular case but also by the introduction of the factor C^2. Since the original KFR rate have been given for the problem of electron detachment of negative ions, it does not include the effect of the long-range Coulomb interaction in the final state. In the atomic case with a pointlike center a simple Coulomb correction factor has been obtained by a WKB approximation of the Coulomb effect,[42] which has been evaluated at the turning point radius to give[14]

$$C^2_{\text{atom}} = \left(\frac{4E_B}{Fr_{\text{atom}}}\right)^{2Z/k_B}, \quad (5)$$

where F is the field amplitude, Z is the charge of the residual ion, and $r_{\text{atom}} = 2/k_B$ with $k_B = \sqrt{2E_B}$ is the turning point of the atomic electron in the bound state. Note that in the above form the Coulomb correction factor equals the ratio in the fore factor between the rates of static field electron detachment[43] and static field ionization[44] (for a more detailed discussion see Ref. 19). Predictions of absolute rates and yields for ionization of hydrogen and noble gas atoms using this Coulomb correction in the KFR formula yield an overall good agreement with results from *ab initio* theories as well as a large range of experimental data.[14] An extension of the above Coulomb factor to the general case of a complex molecule with more than one nuclear center has not been developed up to now. But, for the present case of the C_{60} fullerene and other fullerenes, which have a cagelike geometrical structure of icosahedral symmetry, we have proposed an analogous Coulomb correction,[32] where the radius r_{atom} is simply extended to $R+\delta a$, where $R=6.7$ a.u. is the hard-sphere radius of the C_{60} "cage" (for the neutral fullerene as well as its cations) and $\delta a (\approx 2/k_B)$ is the spill-out radius of the electron cloud (e.g., Ref. 41). This gives for the fullerenes

$$C^2(Z,E_B,F) = \left(\frac{4E_B}{F(R+\delta a)}\right)^{2Z/k_B}. \quad (6)$$

The Coulomb correction factor [as well as its atomic counterpart, Eq. (5)] amplifies the ionization rates at low intensities. In the case of atoms it has been found[14] that the Coulomb corrected KFR formula applies well in the nonperturbative intensity regime, but not at very low intensities in the perturbative multiphoton regime. We further note that C^2 decreases below 1 at very high intensities, in general, well beyond the saturation intensities. In order to prevent an unintentional damping of the ionization rates in this intensity regime one has to require $C^2 \geqslant 1$ at all intensities in the numerical calculations.

The orientation of the C_{60} fullerene in space is determined in Eq. (3) via the set of vectors $\{\boldsymbol{R}_1,\ldots,\boldsymbol{R}_{60}\}$. Results of present calculations are obtained by averaging the ionization rate over the orientation of the fullerene assuming a random orientation of the molecule in the experiment. We may note parenthetically that the ionization rates vary slightly with the orientation of the fullerene. Since experimental data for the rate of ionization are not available, we have determined the ion yield distributions by inserting the calculated ionization rates for different charge states into the rate equations governing the populations (e.g., Ref. 45), integrating them over the pulse profile at a fixed point, and adding the contributions from all the points in the laser focus, in order to compare the theoretical predictions with the experimental observations. Predictions for ion yields as a function of the peak intensity at near-infrared and infrared wavelengths have been given before.[32] In this work we concentrate on the analysis of the experimental data for the saturation intensities.

III. RESULTS AND DISCUSSION

In this section we use the present rate formula, Eq. (3), together with the corresponding rate equations to determine ion yields and saturation intensities of C_{60}^{q+} in ultrashort laser pulses at different wavelengths, namely, 395, 790, 800, 1500, and 1800 nm. While at the lower wavelengths stable ions up to $q=6$ have been observed,[35] using infrared radiation even higher charge states up to C_{60}^{12+} (with reported saturation intensities up to $q=9$) have been detected.[27] Recent theoretical calculations show that the electrostatic Coulomb stability limit of the C_{60} fullerene would be reached at $q=14$.[46] This *static* limit is found to be reduced to $q=12$ (Refs. 47 and 48) in a *dynamical* process, when the higher charge states are produced with an excess vibrational energy upon ionization of C_{60} by a long wavelength laser pulse. We may note that the latter result is in agreement with the experimental observations at 1800 nm.

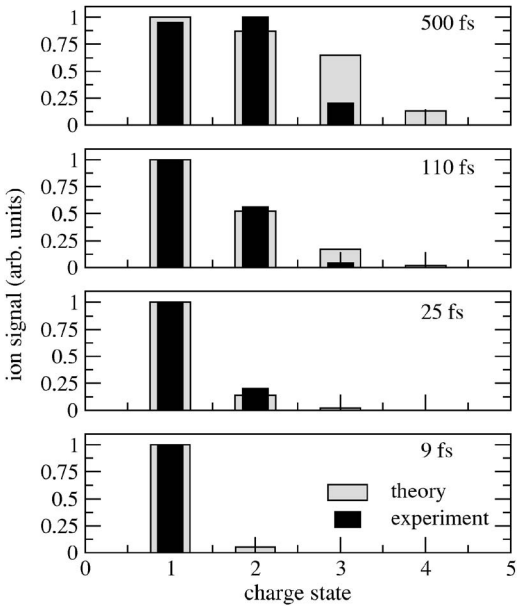

FIG. 1. Comparison of predictions of the present theory (gray bars) for the relative ion yields of different charge states with the corresponding experimental data (black bars, taken from Ref. 35) at several pulse lengths. The peak intensity and the laser wavelength was fixed at 4×10^{13} W/cm^2 and 800 nm, respectively.

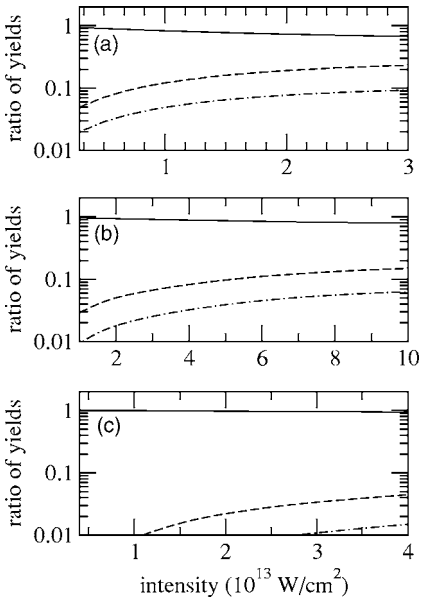

FIG. 2. Contributions of partial ion yields due to ionization from the h_u-HOMO (solid lines) and the h_g (dashed lines) and g_g (dashed-dotted lines) orbitals to the total ion yields as a function of the peak intensity for three laser pulses, (a) $\lambda=395$ nm and $\tau=45$ fs, (b) $\lambda=800$ nm and $\tau=27$ fs, and (c) $\lambda=1500$ nm and $\tau=70$ fs.

We may point out that the present theoretical description of ionization of C_{60} to higher charge states is solely based on sequential (or stepwise) single ionization. Before we proceed we therefore first discuss to which extent the omission of nonsequential ionization and fragmentation processes may influence our results for the saturation intensities presented below. It is well known from experimental and theoretical studies in atoms (see e.g., Refs. 15, 49, and 50) that in the intensity regime close to saturation of ionization of a given charge state the contributions of nonsequential ionization processes are negligible. According to recent experimental observations similar conclusions hold for the ionization of C_{60} too.[30] The degree of fragmentation of the C_{60} fullerene appear to depend on the length of the applied laser pulse. According to experimental observations at 800 nm mostly intact ions with a very small amount of fragments have been observed for pulses up to about 25 fs (e.g., Ref. 35), while at longer pulse durations [40 fs (Ref. 30) or >110 fs (Ref. 35)] significant fragmentation sets in. On the other hand, at infrared wavelengths of 1500 nm and longer there has been almost no fragmentation observed at pulse lengths of 70 fs.[27,30] The onset of fragmentation may be influenced by excitation of intermediate resonances and/or the energy transfer from electronic excitations into nuclear vibrations.[28,47,48]

In order to test the purely sequential treatment for pulses of different durations, we have determined relative ion yields at 800 nm and a constant laser peak intensity of 4×10^{13} W/cm^2 but different pulse lengths. The results of these calculations (gray bars) are compared in Fig. 1 with the experimental data by Shchatsinin *et al.* (black bars, Ref. 35). Please note that both the experimental and the theoretical results for the ion signals are scaled independently at each pulse length such that the maximum ion signal is equal to 1. From the comparison, given on a linear scale, a good agreement between experiment and theory is found at the shortest pulse lengths of 9 and 25 fs. We note an overestimation of the experimental observations by the theoretical predictions for the higher charge states for the longer pulse durations, which might be interpreted as a signature of increase of fragmentation in the experiment.[51] We therefore concentrate below on the analysis of the saturation intensities of the different charge states of C_{60} in ultrashort pulses of a few tens of femtoseconds.

Next, we compare the contributions from different valence shells to the total ion yield of the neutral C_{60} fullerene at several laser wavelengths. This is an important test for the further analysis, since it is known[52–54] that electron emission from molecular orbitals of certain symmetry can be suppressed due to destructive interference effects. As a result it has been predicted[45] that in the case of polyatomic molecules ionization from several valence orbitals, which are energetically close together, can contribute significantly to the total yield. As outlined above, C_{60} has 60 π- and 180 σ-valence electrons which, however, form a distinct energy level structure, where the levels are labeled according to the elements of the symmetry group I_h (e.g. Ref. 29). We have taken into account ionization from the h_u-HOMO ($E_B=7.4$ eV) and the h_g-HOMO-1 ($E_B=9.33$ eV) and g_g-HOMO-2 ($E_B=9.61$ eV), where the ionization potentials are obtained from the Hartree-Fock calculations. The results of our calculations for three laser pulses, namely, (a) at $\lambda=400$ nm and $\tau=45$ fs, (b) $\lambda=800$ nm and $\tau=27$ fs, and (c) $\lambda=1500$ nm and $\tau=70$ fs, are shown in Fig. 2. It is obvious from the comparison that the relative contribution from the HOMO (solid lines) strongly dominates. We may note that the relative ion yields from the inner valence shells increase with increasing laser intensity and frequency. However, for the present interests the contributions from the HOMO-1 and HOMO-2 levels are

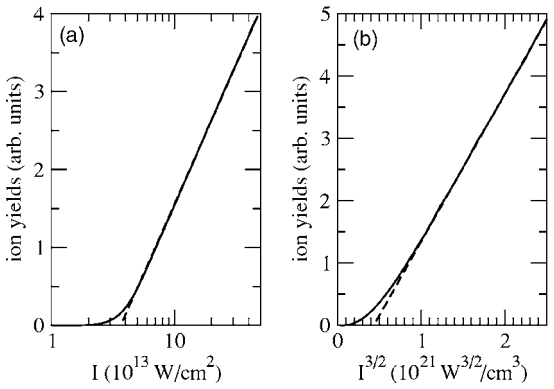

FIG. 3. Determination of the saturation intensity I_{sat} in (a) a cylindrical ($\lambda = 1500$ nm, $\tau = 70$ fs) and (b) a Gaussian focal volume ($\lambda = 800$ nm, $\tau = 27$ fs). For details see text.

insignificant at all wavelengths and intensities investigated. We have performed the same analysis for the ionization of the higher charge states up to C_{60}^{9+} and have found that in all cases electron emission from the HOMO gives the dominant contribution to the total ion yield. Thus, according to the present *S*-matrix study in a sequential ionization scenario the ten electrons from the initial h_u-HOMO will be ionized first before emission from inner valence shells becomes effective.

Now, we turn to the analysis of the experimental data for the saturation intensities obtained at different laser wavelengths. The saturation effect sets in when the ionization probability in the focal region is not considerably less than one.[55,56] There are different techniques for the determination of the saturation intensities in the experiment. We have adopted the procedure proposed by Hankin *et al.*,[16] who have made use of the fact that beyond saturation the ion yields are solely determined by the form of the laser focal volume. We consider the two main forms of focal volumes used in the experiments, namely, a cylindrical and a Gaussian focal volume. In the former case of cylindrical symmetric parallel beam irradiation, the intensity profile across the focal area is constant in the longitudinal direction and of Gaussian shape in the radial direction. On the other hand, a Gaussian focal volume is determined by a Gaussian intensity profile in both, longitudinal and radial, directions of the focal volume. Please note that these definitions specify the spatial beam profile only; for the temporal beam profile we have assumed a Gaussian shape throughout the calculations. It is well known that in case of a cylindrical focal volume the signals are expected to increase as $\log I$ (e.g., Ref. 16) and for a Gaussian focal volume as $I^{3/2}$ (e.g., Ref. 57). By plotting the yields on a linear scale against (a) $\log I$ (for a cylindrical focal volume) and (b) $I^{3/2}$ (for a Gaussian focal volume), as shown in Fig. 3, the saturation intensity is then extracted by extrapolating the high intensity linear part of the ion yields to the intensity axis, either graphically or numerically, and taking the intensity at the intersection point. This method has been proposed by Hankin *et al.*[16] for the cylindrical focal volume and is adopted here for the case of a Gaussian focal volume as well. Indeed, we have tested that using this method one gets almost the same value for the saturation intensity in a cylindrical and in a Gaussian focal volume at

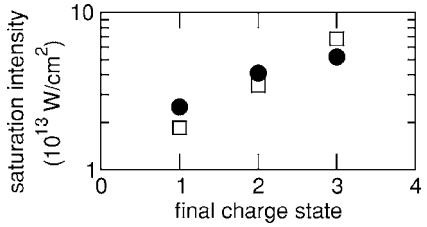

FIG. 4. Comparison of the theoretical predictions for the saturation intensities of C_{60}^{q+} (solid circles) with the experimental data [open squares (Refs. 28 and 33–35)] at a wavelength of 395 nm and a pulse duration of 45 fs.

the same laser parameters, which is a satisfactory result. We note that there are at least two further techniques suggested in the literature how to determine saturation intensities. Both procedures make use of the fact, that in a log-log plot of the ion yields as function of the peak intensity the yields below saturation can be approximately fitted by a power-law dependence as I^s. Therefore, in case of a Gaussian focal volume the saturation intensity can be defined[58] as the intersection of two straight lines in the log-log plot (I^s dependence below and $I^{3/2}$ dependence above saturation). Recently, the I^s dependence has been further used to estimate the saturation intensity via an analytical formula.[35] We may, however, note that the I^s dependence is an approximate empirical observation[59] in contrast to the method explained above, which relies on a well-defined expansion of the focal volume (at least for cylindrical and Gaussian focal volumes). We have tested that the results for the saturation intensities obtained by all these methods are very close to each other.

Next, we compare the theoretical predictions (solid circles) for the saturation intensities of C_{60}^{q+} with the experimental data (open squares) at wavelengths between 395 and 1800 nm in Figs. 4–6. Ionization of atoms and molecules is

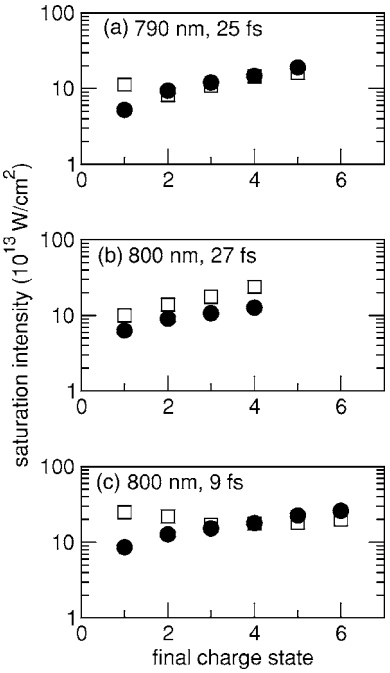

FIG. 5. Same as Fig. 4 but at Ti:sapphire wavelengths (a) 790 nm, 25 fs [experimental data (Refs. 28, 34, and 60)], (b) 800 nm, 27 fs [experimental data (Ref. 35)], and (c) 800 nm, 9 fs [experimental data (Ref. 35)].

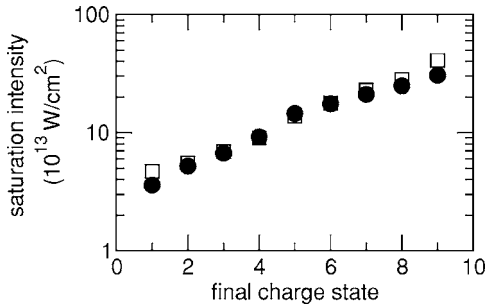

FIG. 6. Same as Fig. 4 but at infrared wavelengths [the lower charge states are determined at 1500 nm, the higher ones at 1800 nm (Ref. 61)] and a pulse duration of 70 fs [experimental data (Ref. 27)].

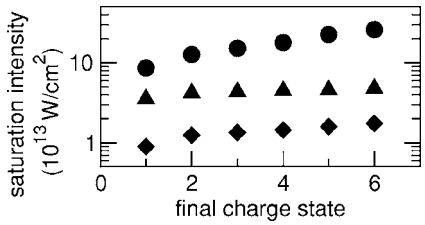

FIG. 7. Comparison of the saturation intensities for the first six charge states of C_{60} at a laser wavelength of 800 nm and a pulse duration of 9 fs. Full calculations (circles), zero-radius approximation (triangles), and incoherent zero-radius approximation (diamonds).

often characterized by the Keldysh parameter $\gamma=\sqrt{E_B/2U_p}$. In this respect our results cover a broad range of wavelengths and intensities from the nonperturbative multiphoton ($\gamma \gg 1$) to the tunnel regime ($\gamma \ll 1$). The comparisons at the second harmonic of the Ti:sapphire laser, $\lambda=395$ nm (Fig. 4, experimental data: Refs. 28 and 33–35), at Ti:sapphire fundamental laser wavelengths (Fig. 5, experimental data: (a) Refs. 28, 34, and 60, (b) and (c) Ref. 35), and the long infrared wavelengths (Fig. 6, experimental data: Ref. 27) show an overall satisfactory agreement.[62] In the short (Fig. 4) and the long wavelength limit (Fig. 6) the theoretical results do not only reproduce the general trend of a monotonic increase of the saturation intensities with increasing charge state in the observations, but are found to quantitatively agree with the experimental data within about 25% or less. A special case appears to be the ionization at the Ti:sapphire laser wavelengths (Fig. 5), since two of the three sets of experimental data show, surprisingly, a decrease of the saturation intensity for the first two [Fig. 5(a)] or the first three charge states [Fig. 5(c)]. This trend is not reproduced by the predictions of the present theory in which a sequential (or stepwise) ionization to higher charge states is assumed. On the other hand there is a very close agreement between theoretical and experimental results for the higher charge states in both cases. We may further note the differences between the experimental data at almost the same pulse length in Fig. 5(a) [25 fs (Refs. 28, 34, and 60)] and Fig. 5(b) [27 fs (Ref. 35)]. The more recently obtained data [Fig. 5(b)] do not show the reversal in the trend with increasing charge states observed earlier and, indeed, the theoretical predictions show a similar increase of the saturation intensities as the experimental data with a slight overall quantitative offset, which may be related to the uncertainty in the calibration of the experimental intensity scale. The origin of the deviation at the shortest pulse length [Fig. 5(c), 9 fs] remains at present unclear. It has to be investigated in future whether effects such as fragmentation or nonsequential ionization, which are not taken into account in the present theory, can explain the differences between experiment and theory for such an ultrashort pulse.

We finally clarify the essential differences in the present *S*-matrix theory which determine the saturation intensities of the C_{60} (and other) fullerenes as compared to the atomic case.[32] As discussed above, the present rate formula, Eq. (3), takes account of the nuclear frame structure of the fullerene, which is characterized by the finite cage radius R as well as the positions of the many nuclear centers, via the Coulomb correction factor, Eq. (6), and the matrix element, Eq. (4). The large radius of the fullerene cage ($R=6.7$ a.u.) apparently reduces the degree of the Coulomb correction and, hence, the ionization rate, as compared to that of a pointlike atomic center ($R=0$). On the other hand, the many nuclear centers in the fullerene lead to a "multi-slit-like" interference of the partial waves arising from the coherent sum of partial amplitudes in the matrix element $M_l(\boldsymbol{k}_N;\boldsymbol{R}_l)$. This is obviously absent for atoms. The latter is a generalization of the molecular "two-slit-like" interference effect, which has been found before to significantly reduce the ionization rate of diatomics having a HOMO of certain symmetry, e.g., π_u-orbital symmetry in case of O_2.[52,54] A similar suppression of the ionization probability via destructive interference is found[32] to be effective in C_{60} (and other fullerenes) too. The suppression by the two effects can be seen from the results of two test calculations. In Fig. 7 we compare the saturation intensities at 800 nm and 9 fs, obtained from the full theory (circles), with those from the "zero-radius" approximation, in which the cage radius in Eq. (6) is set to zero (triangles), and the "incoherent zero-radius" approximation, in which in addition the modulo square of the coherent sum of the partial amplitudes M_l in Eq. (3) has been replaced by the *incoherent* sum of their squares (diamonds). The saturation intensities obtained for the test cases lie invariably below those for the real fullerene counterparts and, therefore, the ionization probabilities are larger, at a given intensity. Thus, the finite cage size and the multi-slit interference mechanism apparently contribute to a suppression of ionization of the Buckminster fullerene and its ions.

IV. SUMMARY

Theoretical analysis of the ionization of C_{60} fullerene and its cations in ultrashort intense laser pulses using the strong-field *S*-matrix theory has been presented. C_{60} with its high symmetry and well defined electronic structure is an interesting prototype to test the applicability of theoretical approaches, used for laser induced ionization of atoms and small molecules before, to large complex molecules. To this end we have, respectively, modified the well-known Keldysh-Faisal-Reiss theory for atoms to the fullerene case by taking account of the icosahedral structural symmetry, the finite size of the fullerene cage, and the multicenter nuclear positions of the C_{60} fullerene in the *S*-matrix amplitude. Fur-

ther, we have proposed a simple extension of the Coulomb correction factor, used in the atomic KFR theory before, to molecules having a cagelike geometrical structure.

This *S*-matrix theory has been then applied to analyze the unexpectedly high saturation intensities of C_{60} and its ions observed in recent experiments and the related effect of suppression of ionization of the fullerene as compared to its companion atom having the same ionization potential. In order to compare the theoretical predictions with the experimental data, ion yields are calculated by employing the *S*-matrix rates in the rate equations using the experimental spatial and temporal laser profiles. Different techniques to determine the saturation intensities have been discussed and used to obtain the respective theoretical predictions for the different charge states.

The results for the saturation intensities are found to be in a good overall agreement with the experimental observations over a broad wavelength regime from 395 to 1800 nm at different pulse lengths. Especially, the results at the second harmonic of the Ti:sapphire laser and at the long infrared wavelengths quantitatively reproduce the experimental observations of a monotonic increase of the saturation intensities with increasing charge state. Deviations between theory and experiment in the trend for the first two charge states as well as the close agreement for the higher charges states at the Ti:sapphire wavelength are discussed.

Further analysis of our results has revealed that independent of the wavelength the contribution from the h_u-HOMO to the ion yields strongly dominates over those from the inner valence orbitals h_g and g_g. Thus, our results indicate that ionization of C_{60} to high charge states dominantly proceeds via sequential removal of electrons, one after the other, from the h_u-HOMO. The influence of nonsequential ionization and fragmentation has been discussed and appear to be negligible near saturation of ionization in laser pulses shorter than about 100 fs.

Finally, we have shown that the suppression of ionization of the C_{60} fullerene and its multiply charged ions, as observed experimentally via unexpectedly high saturation intensities, can be well explained within the present single active electron *S*-matrix theory as being induced by the finite cage size of the fullerene and a multi-slit-like interference effect between partial waves emitted from the different nuclei of the fullerene.

ACKNOWLEDGMENTS

The authors thank I. V. Hertel, T. Laarmann, C. P. Schulz, V. R. Bhardwaj, P. B. Corkum, and D. M. Rajner for sending their experimental data in numerical form and fruitful discussions. The authors further acknowledge fruitful discussion with H. Kono, which have been partially provided by the support via the Core-to-Core Program *Ultrafast Intense Laser Science* (JSPS, Japan). One of the authors (A.J.-B.) acknowledges partial support from EC Human Potential Programme under Contract No, HPRN-CT-2002-00209. One of the authors (A.B.) acknowledges partial support from NSERC Canada via SRO Grant No. 5796-299409/03. This work was further partially supported by the National Science Foundation through a grant for the Institute for Theoretical Atomic, Molecular, and Optical Physics at Harvard University and Smithsonian Astrophysical Observatory.

[1] R. Judson and H. Rabitz, Phys. Rev. Lett. **68**, 1500 (1992).
[2] A. Assion, T. Baumert, M. Bergt, T. Brixner, B. Kiefer, V. Seyfried, M. Strehle, and G. Gerber, Science **282**, 919 (1998).
[3] R. J. Levis, G. M. Menkir, and H. Rabitz, Science **292**, 709 (2001).
[4] K. C. Kulander, Phys. Rev. A **38**, 778 (1988).
[5] B. Walker, B. Sheehy, L. F. DiMauro, P. Agostini, K. J. Schafer, and K. C. Kulander, Phys. Rev. Lett. **73**, 1227 (1994).
[6] R. Shakeshaft, R. M. Potvliege, M. Dörr, and W. E. Cocke, Phys. Rev. A **42**, 1656 (1990).
[7] L. Dimou and F. H. M. Faisal, Phys. Lett. A **171**, 211 (1992).
[8] L. V. Keldysh, Zh. Eksp. Teor. Fiz. **47**, 1945 (1964) [Sov. Phys. JETP **20**, 1307 (1965)].
[9] A. M. Perelomov, S. V. Popov, and M. V. Terent'ev, Zh. Eksp. Teor. Fiz. **50**, 1393 (1966) [Sov. Phys. JETP **23**, 924 (1966)].
[10] M. V. Ammosov, N. B. Delone, and V. P. Krainov, Zh. Eksp. Teor. Fiz. **91**, 2008 (1986) [Sov. Phys. JETP **64**, 1191 (1986)].
[11] F. H. M. Faisal, J. Phys. B **6**, L89 (1973).
[12] H. R. Reiss, Phys. Rev. A **22**, 1786 (1980).
[13] S. F. J. Larochelle, A. Talebpour, and S. L. Chin, J. Phys. B **31**, 1215 (1998).
[14] A. Becker, L. Plaja, P. Moreno, M. Nurhuda, and F. H. M. Faisal, Phys. Rev. A **64**, 023408 (2001).
[15] S. F. J. Larochelle, A. Talebpour, and S. L. Chin, J. Phys. B **31**, 1201 (1998).
[16] S. M. Hankin, D. M. Villeneuve, P. B. Corkum, and D. M. Rayner, Phys. Rev. Lett. **84**, 5082 (2000).
[17] S. M. Hankin, D. M. Villeneuve, P. B. Corkum, and D. M. Rayner, Phys. Rev. A **64**, 013405 (2001).
[18] A. Becker and F. H. M. Faisal, J. Phys. B **29**, L197 (1996).
[19] A. Becker and F. H. M. Faisal, J. Phys. B **38**, R1 (2005).
[20] A. Becker, R. Dörner, and R. Moshammer, J. Phys. B **38**, S753 (2005).
[21] C. Ruiz, L. Plaja, L. Roso, and A. Becker, Phys. Rev. Lett. **96**, 053001 (2006).
[22] G. N. Gibson, R. R. Freeman, and T. J. McIllrath, Phys. Rev. Lett. **67**, 1230 (1991).
[23] S. L. Chin, Y. Liang, J. E. Decker, F. A. Ilkov, and M. V. Ammosov, J. Phys. B **25**, L249 (1992).
[24] T. D. G. Walsh, J. E. Decker, and S. L. Chin, J. Phys. B **26**, L85 (1994).
[25] T. D. G. Walsh, F. A. Ilkov, J. E. Decker, and S. L. Chin, J. Phys. B **27**, 3767 (1994).
[26] A. Talebpour, C.-Y. Chien, and S. L. Chin, J. Phys. B **29**, L677 (1996).
[27] V. R. Bhardwaj, P. B. Corkum, and D. M. Rayner, Phys. Rev. Lett. **91**, 203004 (2003).
[28] I. V. Hertel, T. Laarmann, and C. P. Schulz, Adv. At., Mol., Opt. Phys. **50**, 219 (2005).
[29] M. S. Dresselhaus, G. Dresselhaus, and P. C. Eklund, *Science of Fullerenes and Carbon Nanotubes* (Academic, New York, 1996).
[30] V. R. Bhardwaj, P. B. Corkum, and D. M. Rajner, Phys. Rev. Lett. **93**, 043001 (2004).
[31] Th. Brabec, M. Coté, P. Boulanger, and L. Ramunno, Phys. Rev. Lett. **95**, 073001 (2005).
[32] A. Jaroń-Becker, A. Becker, and F. H. M. Faisal, Phys. Rev. Lett. **96**, 143006 (2006).
[33] M. Tchaplyguine, K. Hoffmann, O. Dühr, H. Hohmann, G. Korn, H. Rottke, M. Wittmann, I. V. Hertel, and E. E. B. Campbell, J. Chem. Phys. **112**, 2781 (2000).
[34] K. Hoffmann, Ph.D. thesis, Freie Universität Berlin, 2000.
[35] I. V. Shchatsinin, T. Laarmann, G. Stibenz, G. Steinmeyer, A. Stalmoshonak, N. Zhavoronkov, C. P. Schulz, and I. V. Hertel, J. Chem. Phys. **125**, 194320 (2006).
[36] D. M. Volkov, Z. Phys. **94**, 250 (1935).
[37] GAUSSIAN03, Revision C.02, Gaussian, Inc., Wallingford, CT, 2004; (http://www.gaussian.com).
[38] D. Porezag, Th. Frauenheim, Th. Köhler, G. Seifert, and R. Kaschner, Phys. Rev. B **51**, 12947 (1995).
[39] G. Seifert, D. Porezag, and Th. Frauenheim, Int. J. Quantum Chem. **58**, 185 (1996).
[40] M. Elstner, D. Porezag, G. Jungnickel, J. Elsner, M. Haugk, Th. Frauenheim, S. Suhai, and G. Seifert, Phys. Rev. B **58**, 7260 (1998).

[41] C. Yannouleas and U. Landman, Chem. Phys. Lett. **217**, 175 (1994).
[42] V. P. Krainov, J. Opt. Soc. Am. B **14**, 425 (1997).
[43] Yu. N. Demkov and G. F. Drukarev, Zh. Eksp. Teor. Fiz. **47**, 918 (1964) [Sov. Phys. JETP **20**, 614 (1965)].
[44] B. M. Smirnov and M. I. Chibisov, Zh. Eksp. Teor. Fiz. **49**, 841 (1965) [Sov. Phys. JETP **22**, 585 (1965)].
[45] A. Jaroń-Becker, A. Becker, and F. H. M. Faisal, Phys. Rev. A **69**, 023410 (2004).
[46] S. Diaz-Tendero, M. Alcami, and F. Martin, Phys. Rev. Lett. **95**, 013401 (2005).
[47] R. Sahnoun, K. Nakai, Y. Sato, H. Kono, Y. Fujimura, and M. Tanaka, Chem. Phys. Lett. **430**, 167 (2006).
[48] R. Sahnoun, K. Nakai, Y. Sato, H. Kono, Y. Fujimura, and M. Tanaka, J. Chem. Phys. **125**, 184306 (2006).
[49] A. Becker and F. H. M. Faisal, Phys. Rev. A **59**, R1742 (1999).
[50] A. Becker and F. H. M. Faisal, Phys. Rev. A **59**, R3182 (1999).
[51] We may note parenthetically that the discrepancies could arise also due to variations in the peak intensities in the experiment.
[52] J. Muth-Böhm, A. Becker, and F. H. M. Faisal, Phys. Rev. Lett. **85**, 2280 (2000).
[53] J. Muth-Böhm, A. Becker, S. L. Chin, and F. H. M. Faisal, Chem. Phys. Lett. **337**, 313 (2001).
[54] F. Grasbon, G. G. Paulus, S. L. Chin, H. Walther, J. Muth-Böhm, A. Becker, and F. H. M. Faisal, Phys. Rev. A **63**, 041402 (2003).
[55] S. L. Chin, N. R. Isenor, and M. Young, Phys. Rev. **188**, 7 (1969).
[56] S. L. Chin and N. R. Isenor, Can. J. Phys. **48**, 1445 (1970).
[57] M. R. Cervenan and N. R. Isenor, Opt. Commun. **13**, 175 (1975).
[58] T. D. G. Walsh, J. E. Decker, and S. L. Chin, J. Phys. B **26**, L85 (1993).
[59] The exponent s is, in general, undetermined in the *nonperturbative* intensity regime (i.e., e.g., above about 10^{12} W/cm^2 for near-infrared frequencies). At low intensities, at which the lowest-order perturbation theory is applicable s is equal to the minimum number of photons needed to overcome the ionization potential. This theoretical result is, however, no longer valid as soon as above threshold ionization (ATI) sets in. Saturation of ionization of atoms and molecules usually appears in the ATI intensity regime.
[60] E. E. B. Campbell, K. Hoffmann, H. Rottke, and I. V. Hertel, J. Chem. Phys. **114**, 1716 (2001).
[61] V. R. Bhardwaj (private communication).
[62] We have included the previously published (Ref. 32) comparison at the infrared wavelengths here for the sake of completeness.